

T-CIL: Temperature Scaling using Adversarial Perturbation for Calibration in Class-Incremental Learning

Seong-Hyeon Hwang Minsu Kim Steven Euijong Whang*
KAIST

{sh.hwang, ms716, swang}@kaist.ac.kr

Abstract

We study model confidence calibration in class-incremental learning, where models learn from sequential tasks with different class sets. While existing works primarily focus on accuracy, maintaining calibrated confidence has been largely overlooked. Unfortunately, most post-hoc calibration techniques are not designed to work with the limited memories of old-task data typical in class-incremental learning, as retaining a sufficient validation set would be impractical. Thus, we propose T-CIL, a novel temperature scaling approach for class-incremental learning without a validation set for old tasks, that leverages adversarially perturbed exemplars from memory. Directly using exemplars is inadequate for temperature optimization, since they are already used for training. The key idea of T-CIL is to perturb exemplars more strongly for old tasks than for the new task by adjusting the perturbation direction based on feature distance, with the single magnitude determined using the new-task validation set. This strategy makes the perturbation magnitude computed from the new task also applicable to old tasks, leveraging the tendency that the accuracy of old tasks is lower than that of the new task. We empirically show that T-CIL significantly outperforms various baselines in terms of calibration on real datasets and can be integrated with existing class-incremental learning techniques with minimal impact on accuracy.

1. Introduction

Nowadays it is essential for deep neural networks to deliver not only precise predictions, but also trustworthy confidence levels indicating the likelihood that predictions are correct. However, with the enhancement of the model’s capabilities, there is a tendency for the model to exhibit excessive confidence in its predictions compared to the actual accuracy [13]. This discrepancy between the confidence levels of the model and the actual accuracy makes model

predictions unreliable to use for decision making. The discrepancy also results in severe failures in real-world safety-critical applications that require reliable models such as autonomous driving [12] and medical diagnostics [15].

With the growing need for reliable models, confidence calibration [13], which adjusts confidence levels of the model to match their actual accuracies, has gained increasing attention. To enhance the calibration of deep neural networks, both post-hoc and training-time methods have been introduced. Post-hoc methods adjust the confidence levels of a model after training by applying a calibration function to the predictions made on a hold-out validation set, such as temperature scaling [13] or histogram binning [41]. Training-time methods refine model calibration during the training phase by altering the loss function [27], implementing label smoothing [36], or using Mixup [43] training on interpolated data samples.

However, conventional post-hoc calibration approaches struggle in class-incremental learning scenarios, where models must continuously adapt to new classes with sufficient data while retaining performance on previously learned classes. Existing works for class-incremental learning [3, 25, 34, 38, 39, 46] focus on preventing catastrophic forgetting [26], losing knowledge of old tasks as they learn new ones. They often assume a limited memory size for old classes, as storing all data may be impractical due to memory constraints and privacy concerns. For post-hoc approaches, the primary challenge stems from this memory limitation. This limitation restricts the retention of a sufficient validation set from old tasks. If a portion of the stored data is reserved solely for validation and excluded from training, model accuracy on old tasks will likely decline due to the reduced amount of training data.

To effectively calibrate models in class-incremental learning, we propose T-CIL, a novel temperature scaling approach that operates without validation data from old tasks (see Figure 1). While exemplars from memory are the only available source of information for old tasks, directly using them for temperature optimization yields abnormally small values due to their use in training. Thus, we optimize

*Corresponding Author

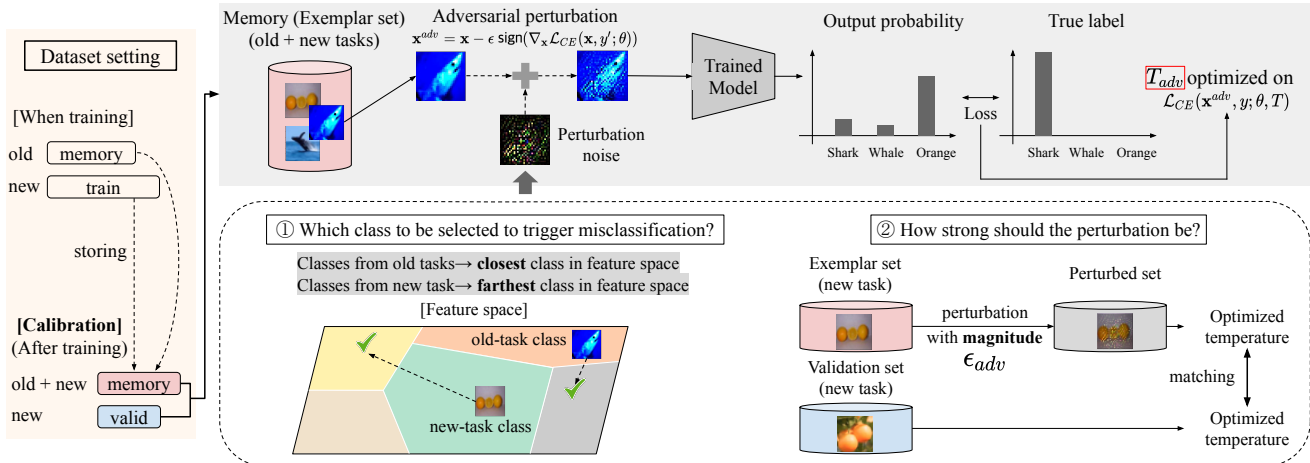


Figure 1. Overview of our proposed framework, T-CIL, a post-hoc calibration framework for class-incremental learning when a validation set only from the new task is available with memory. Our method leverages exemplars from memory by applying adversarial perturbations, whose direction and magnitude are determined based on feature distance and new task validation data, respectively. The temperature is then optimized using these perturbed exemplars.

the temperature on adversarially perturbed exemplars. We introduce adversarial perturbation of exemplars, designed with two key components: *direction* and *magnitude*.

The key idea of T-CIL is to perturb exemplars more strongly for old tasks than for the new task by adjusting the perturbation direction based on feature distance, with the magnitude determined using the new-task validation set. While the perturbation levels can be controlled simply with two magnitude parameters for old and new tasks, determining the proper magnitude for old tasks is unrealistic without a validation set, as it is impossible to know how much the magnitude affects temperature optimization exactly. Therefore, we use a single magnitude determined using a new-task validation set and adjust the levels by setting the perturbation direction using target class selection. Since old tasks generally exhibit lower test accuracy than new tasks, we induce easier mispredictions on exemplars from old tasks than new task with the same magnitude. T-CIL is guiding the model to misclassify old-task data into their closest classes in feature space, while mispredicting new-task data into the farthest classes. This strategy makes the perturbation magnitude computed from the new task also applicable to old tasks, leveraging the tendency that the accuracy of old tasks is lower than that of the new task.

We perform comprehensive experiments on various image classification datasets in class-incremental learning settings. We demonstrate the effectiveness of T-CIL in terms of confidence calibration while minimally changing accuracy without a validation data from old tasks. We show that T-CIL consistently outperforms existing post-hoc calibration methods and can be integrated with any class-incremental learning technique. Even if there is enough data to construct a validation set, this may result in a tradeoff in accu-

racy, which T-CIL does not have. For instance, when using Experience Replay (ER) [6] with 100% of the memory for training exemplars, instead of reserving 25% for validation, we observe an improvement in average accuracy on CIFAR-100 from 53.56% to 56.25%. This performance gain is comparable to the accuracy improvement achieved by EEIL [3] (a method specifically designed to mitigate forgetting) over ER, but with the significant advantage of not requiring an additional old-task validation set. See Section 6.2 for more details.

Summary of Contributions: (1) We propose a new post-hoc calibration method, called T-CIL, specifically designed for class-incremental learning; (2) We introduce a novel temperature optimization approach using adversarially perturbed exemplars without a validation set from old tasks; (3) We demonstrate the effectiveness of T-CIL through comprehensive experiments, showing superior calibration performance and compatibility across various class-incremental learning methods.

2. Related Work

Confidence Calibration The purpose of confidence calibration is to narrow the discrepancy between a model’s accuracy and its confidence levels. Existing calibration works can be categorized into two main types: training-time methods and post-hoc methods. Training-time methods consider calibration during model training. Using other types of loss functions instead of a vanilla cross-entropy loss are considered training-time methods [10, 27]. Implicit regularizations are also widely used during training including label smoothing [24, 31, 36] and Mixup [29, 43].

In comparison, our focus is on post-hoc approaches where the model’s output logits are adjusted after training

while preserving the order of predicted classes. Post-hoc methods include Platt scaling [33], histogram binning [41], dirichlet scaling [20], isotonic regression [42]. In particular, temperature scaling [13] is a technique that scales the model’s output logits using a temperature parameter determined on a validation set and is known to be effective in in-distribution contexts. Many variants [9, 16, 44] of temperature scaling have also been proposed. However, the performance of temperature scaling deteriorates in out-of-distribution scenarios. Despite this challenge, temperature scaling has been utilized in various settings including distribution shifts [30], distribution overlaps [7], multi-domain [40], out-of-domain [8], and domain drift situations [37]. More recently, [23] is the first calibration study in continual learning that uses some of the above existing methods along with an old-task validation set. All of these works assume access to the information of all classes via a validation set. In comparison, we assume that the validation set only contains data for classes from the new task and that any data from old tasks is unavailable. Under this condition, T-CIL is the first effective temperature scaling without a validation set from old tasks.

Class-Incremental Learning (CIL) Class-incremental learning [4, 21, 46, 47] is a type of continual learning in which new tasks are learned sequentially, each with unique sets of classes. The main objective in class-incremental learning research is to mitigate the catastrophic forgetting problem to maintain accuracy across tasks. From a data-centric perspective, some studies use a small number of exemplars from old tasks [1, 6] to adjust the directions of the gradient [5, 25] or apply knowledge distillation [3, 34, 38, 45]. For an architecture perspective, dynamic architecture expansion approaches [39] have been proposed. A particular study [17] addresses model confidence within class-incremental learning, focusing mainly on the confidence of the latest task rather than the older ones. In contrast, our study focuses on recalibrating the confidence of both old and new tasks. While existing class-incremental learning approaches often overlook confidence calibration, T-CIL specifically addresses this crucial aspect.

3. Preliminaries

Notation for CIL Suppose we are at the t -th incremental task in an offline class-incremental learning setting. Let $C_{t,old} = \sum_{j=1}^{t-1} C_j$ denote the number of classes from old tasks, where C_j is the number of classes at j -th task, and C_t represents the number of classes in the new task. We train a model to classify an image into a total of $C_{t,old} + C_t$ classes, combining both old and new tasks.

We consider a scenario after the model training at the t -th incremental task, as our focus is on the post-hoc process. Before training, we have a dataset of the new task,

$\mathcal{D}_t = \{(\mathbf{x}_i, y_i)\}$, where $\mathbf{x}_i \in \mathcal{X}_t$ is an input sample and $y_i \in \mathcal{Y}_t = \{C_{t,old} + 1, \dots, C_{t,old} + C_t\}$ is its corresponding label. Also we obtain a memory set from the $t - 1$ -th task, $\mathcal{M}_{t-1} = \{(\mathbf{x}_j, y_j)\}$, containing a subset of data (exemplars) from old tasks, where $y_j \in \{1, \dots, C_{t,old}\}$. We split \mathcal{D}_t into a training set, $\mathcal{D}_{t,train}$, and a small validation set $\mathcal{D}_{t,valid}$. The memory is significantly smaller than the training set for the new task, such that $|\mathcal{D}_{t,train}|/C_t \gg |\mathcal{M}_{t-1}|/C_{t,old}$. When training the t -th task, we use both $\mathcal{D}_{t,train}$ and \mathcal{M}_{t-1} . After training, we update the memory, denoted as \mathcal{M}_t , by storing a portion of $\mathcal{D}_{t,train}$ in it. Calibration is then performed using $\mathcal{D}_{t,valid}$ and \mathcal{M}_t , which contains data from both old and new tasks.

Notation for Calibration Let f_θ be a classifier with parameters θ . f_θ outputs a logit $\mathbf{z}_i = f_\theta(\mathbf{x}_i)$, where $f_\theta : \mathcal{X} \rightarrow \mathbb{R}^K$ with dimension $K = C_{t,old} + C_t$. Let \mathcal{L} be the loss function that measures how well the model’s predictions $f_\theta(\mathbf{x}_i)$ matches the true label y_i . Especially, \mathcal{L}_{CE} is the cross-entropy loss on a sample (\mathbf{x}_i, y_i) defined as:

$$\mathcal{L}_{CE}(\mathbf{x}_i, y_i; \theta) = - \sum_{k=1}^K y_{i,k} \log p_{i,k} \quad (1)$$

where $p_{i,k} = \frac{e^{z_{i,k}}}{\sum_{j=1}^K e^{z_{i,j}}}$ is the output probability of the k -th class for the i -th input calculated by applying the softmax function to the logit \mathbf{z}_i . $\hat{p}_i = \max_k p_{i,k}$ is the confidence level, and $\hat{y}_i = \arg \max_k p_{i,k}$ is the predicted class of \mathbf{x}_i .

To measure how well a model is calibrated, we introduce the Expected Calibration Error (ECE) [28] defined as $\mathbb{E}_{(\mathbf{x}_i, y_i) \sim \mathcal{P}} [|P(\hat{y}_i = y_i | \hat{p}_i) - \hat{p}_i|]$. In practice, with a finite test set, we divide the interval $[0, 1]$ into B equal-width bins, where B_i is the i -th bin representing the interval $(\frac{i-1}{B}, \frac{i}{B}]$. We compute the average accuracy, $acc(B_i) = \frac{1}{|B_i|} \sum_{j \in B_i} \mathbb{1}(\hat{y}_j = y_j)$, where $\mathbb{1}(\cdot)$ is an indicator function, and the average confidence, $conf(B_i) = \frac{1}{|B_i|} \sum_{j \in B_i} \hat{p}_j$. Then, ECE is calculated as $\sum_{i=1}^B \frac{|B_i|}{N} |acc(B_i) - conf(B_i)|$, where the N is the test data size used for evaluation. A lower ECE indicates better calibration.

Temperature Scaling Temperature scaling [13] is a widely used post-hoc calibration technique that assumes a validation set. The classifier’s output logits are scaled by a temperature value $T > 0$.

$$T^* = \arg \min_T \mathcal{L}_{CE}(\mathbf{x}, y; \theta, T) \quad (2)$$

$$\mathcal{L}_{CE}(\mathbf{x}, y; \theta, T) = - \frac{1}{N} \sum_{i=1}^N \sum_{k=1}^K y_{i,k} \frac{e^{z_{i,k}/T}}{\sum_{j=1}^K e^{z_{i,j}/T}} \quad (3)$$

If T is large, the output probability distribution would be flattened into a uniform distribution; a small T would

sharpen the probability distribution instead. The optimal temperature is determined as the temperature that minimizes the cross-entropy loss on a validation set.

Adversarial Perturbation Adversarial perturbations add adversarial noise to input data to intentionally trigger misclassification. The Fast Gradient Sign Method (FGSM) [11] is an effective method for generating such perturbations. FGSM generates noise that maximizes the model’s loss value for the given data and adds this noise to the data. FGSM perturbs a datapoint \mathbf{x} in two ways, depending on whether a target class for misclassification is specified:

$$\mathbf{x}^{adv} = \mathbf{x} + \epsilon \text{sign}(\nabla_{\mathbf{x}} \mathcal{L}_{CE}(\mathbf{x}, y; \theta)) \quad (4)$$

$$\mathbf{x}^{adv} = \mathbf{x} - \epsilon \text{sign}(\nabla_{\mathbf{x}} \mathcal{L}_{CE}(\mathbf{x}, y'; \theta)) \quad (5)$$

where ϵ is the magnitude of the perturbation, $\text{sign}(\cdot)$ is the sign function, y is the true label, and y' is the target class different from y to induce a misclassification.

4. Temperature Bias in CIL

We investigate the calibration bias of temperature scaling when only new-task data is available for validation in class-incremental learning. While existing variants of temperature scaling address challenging scenarios like domain or distribution shifts with constrained validation sets, they still assume access to information from all classes via the validation set. In our setting, despite a consistent domain (image data), the validation set exclusively contains data from the new task, excluding any data from old tasks.

To verify the effectiveness of temperature scaling in this setting, we conduct experiments on two real-world image datasets: CIFAR-100 and Tiny-ImageNet. For CIFAR-100, we divide the dataset into 10 incremental tasks with 10 classes per task and train a 32-layer ResNet [14] model. For Tiny-ImageNet, we train a ResNet-18 model with 10 tasks and 20 classes per task. In both cases, we employ Experience Replay (ER) [6] as our base learning technique.

After training, we optimize temperatures using two different sets: (1) a validation set containing data only from the new task, and (2) a test set containing data from all tasks (optimal). As shown in Figure 2, the gap between these optimized temperatures increases as the tasks progress. This observation suggests that using temperature optimized solely on new task validation data leads to poorer calibration performance on the actual test set, which includes data from both old and new tasks. This comparison highlights the potential bias when using only new-task data for temperature optimization.

5. Method

In this section, we introduce T-CIL, a novel post-hoc calibration method specifically designed for class-incremental

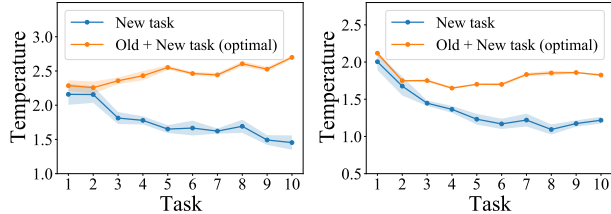


Figure 2. Temperatures after training each task using ER method on the CIFAR-100 (left), and Tiny-ImageNet (right) datasets. For each task, we show two different temperatures: (1) optimized on a validation set containing only new-task data, and (2) the optimal temperature obtained on the test set across all tasks.

learning when a validation set only from the new task is available. T-CIL addresses the challenge of limited access to old-task data by leveraging adversarially perturbed exemplars. We propose an adversarial perturbation approach composed of perturbation direction and magnitude. While one may use other augmentation techniques like Mixup for post-hoc calibration, adversarial perturbation is a more effective method to use because we need transformed old-task exemplars with degraded accuracy for calibration and adversarial perturbation serves the purpose directly. The full T-CIL algorithm is also presented in Section 5.3.

5.1. Perturbation Direction Policy

To address the absence of a validation set from old tasks, we leverage exemplars from memory to gain information about old tasks. However, directly using these exemplars for temperature tuning leads to overfitting and inaccurate temperature estimates. This is because the model has already encountered these exemplars during training and tends to overfit on this limited data, resulting in high-confidence outputs and near-perfect accuracy. In fact, as shown in Figure 3, the model accuracy on exemplars is almost 100% on the CIFAR-100, regardless of whether the learning technique is Experience Replay (ER) or Dynamically Expandable Representation (DER) [39], which preserves the old task accuracy using a dynamic architecture.

This near-perfect accuracy disrupts the temperature optimization process, as described in Equation 2. Temperature optimization aims to find the temperature that minimizes the cross-entropy loss. When most predictions are correct, this process tends to lower the temperature, pushing confidence levels closer to 1. Consequently, using exemplars directly results in an abnormally low temperature, hindering calibration performance on the test set.

Thus, we perturb the exemplars adversarially triggering mispredictions to reduce overfitting for temperature optimization. Each perturbation of an exemplar has a direction and a magnitude. All perturbations have the same magnitude, which is configured with the parameter ϵ_{adv} . While we could use separate magnitude parameters for old and

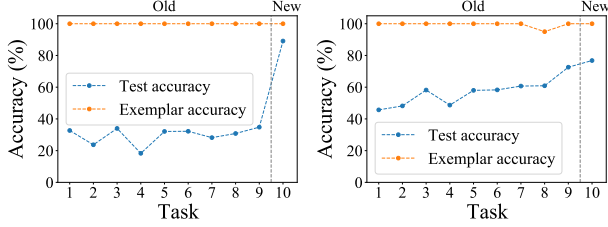


Figure 3. Task-wise accuracy comparison after completing training on the final (10th) task of CIFAR-100 dataset using Experience Replay (ER) (*left*), and Dynamically Expandable Representation (DER) [39] (*right*).

new tasks, determining the right magnitude for the old tasks is not easy without any validation data to tell us how the magnitude influences the temperature optimization. Thus we only employ a single magnitude value that is established using the validation data from the new tasks. We explain how to derive the magnitude in Section 5.2.

With the single magnitude, we perturb exemplars more strongly for old tasks than for the new task by adjusting the perturbation direction via target class selection. For exemplars from old tasks, we select the easiest target classes to induce errors, while for new task exemplars, we select the hardest target classes. This idea is based on the tendency that the accuracy of old tasks is lower than that of the new task as shown in Figure 3. The results show that models after training the 10th task tend to perform better on new tasks, where more training data is available.

We use feature distance within the feature space as an indicator of how easily an exemplar can cause mispredictions for different target classes, where the farthest class represents the most difficult target, and the nearest class represents the easiest target as represented in Figure 4. To measure the feature distance, we decompose the classifier f_θ as $f_\theta(\cdot) = g_w(\phi_v(\cdot))$, where $\theta = \{w, v\}$, $\phi_v(\cdot)$ is the feature extractor with parameters v , and $g_w(\cdot)$ is the classification layer with parameters w . For each exemplar $\mathbf{x}_e \in \mathcal{M}_t$, where \mathcal{M}_t contains exemplars from both old and new tasks, we compute the L2 distance between its feature $\phi_v(\mathbf{x}_e)$ and the mean of features for each class $\mu_c = \frac{1}{|X_c|} \sum_{\mathbf{x}_e \in X_c} \phi_v(\mathbf{x}_e)$, where X_c is the set of exemplars of each class $c \in \{1, \dots, C_{t,old} + C_t\}$. The target label y'_e of data point (\mathbf{x}_e, y_e) is then defined as follows:

$$y'_e = \begin{cases} \arg \max_{c, c \neq y_e} \|\phi_v(\mathbf{x}_e) - \mu_c\| & \text{if } y_e \in \mathcal{Y}_t \\ \arg \min_{c, c \neq y_e} \|\phi_v(\mathbf{x}_e) - \mu_c\| & \text{if } y_e \notin \mathcal{Y}_t \end{cases} \quad (6)$$

where $\mu_c = \frac{1}{|X_c|} \sum_{\mathbf{x}_e \in X_c} \phi_v(\mathbf{x}_e)$

Then, we perturb exemplars to force the model directly to predict to the target class by using Equation 5. This approach minimizes the loss concerning a chosen target class,

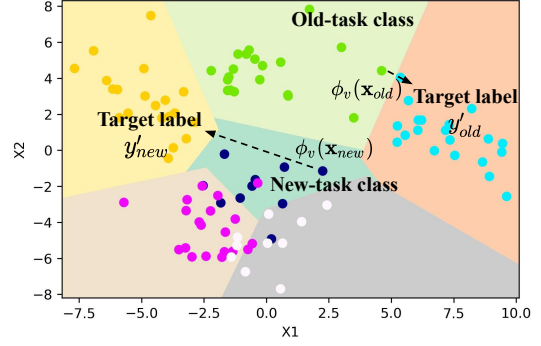


Figure 4. A perturbation direction policy of T-CIL visualized on a two-dimensional feature space with decision boundaries. For old-task data, the target class is selected based on the closest distance in feature space, while for the new-task data, the farthest class is selected based on maximum distance in the feature space.

thus actively pushing the model to misclassify the perturbed exemplars intentionally. We denote the resulting perturbed exemplar set as \mathcal{M}_t^{adv} . The optimized temperature, T_{adv} , is then determined by minimizing the cross-entropy loss on these adversarially perturbed exemplars as follows:

$$T_{adv} = \arg \min_T \mathcal{L}_{CE}(\mathbf{x}_e^{adv}, y_e; \theta, T) \quad (7)$$

$$\mathbf{x}_e^{adv} = \mathbf{x}_e - \epsilon \text{sign}(\nabla_{\mathbf{x}_e} \mathcal{L}_{CE}(\mathbf{x}_e, y'_e; \theta)) \quad (8)$$

where \mathbf{x}_e^{adv} represents the perturbed exemplar data, y'_e is the target class of perturbation, y_e is the original label of \mathbf{x}_e , and ϵ is the magnitude of perturbation.

We provide supporting experiments on why it makes sense for T-CIL to perturb old-task exemplars towards closer classes to match the lower real accuracy. Using T-CIL with ER on CIFAR-100 and comparing results after training up to the 5th and 10th tasks (see Section 6 for the setup details), the accuracy gap between old and new tasks increases from 38% to 60%. At the same time, T-CIL’s misprediction rate gap increases from 17.8% to 43.7%, which is proportional to the accuracy gap increase.

5.2. Perturbation Magnitude Search

We determine the perturbation magnitude parameter ϵ_{adv} using a new-task validation set, since existing works [2, 11] for adversarial perturbation determine the magnitude heuristically as a hyperparameter. ϵ_{adv} is selected to yield a temperature on perturbed exemplars that matches the optimal temperature from the new-task validation set.

Initially, we determine a target temperature by minimizing the cross-entropy loss on $\mathcal{D}_{t,valid}$, a validation set from the new task. We find the magnitude of perturbation, ϵ_{adv} that results in this target temperature when applied to perturbations on $\mathcal{M}_{t,new}$, the exemplar set from the new task. Note that $\mathcal{M}_{t,new}$ is sampled from $\mathcal{D}_{t,train}$ after training,

Algorithm 1: The T-CIL algorithm.

Input: Exemplar set \mathcal{M}_t , validation set from new task $\mathcal{D}_{t,valid}$, model parameters $\theta = \{w, v\}$, tolerance δ

```
1 /* At the  $t$ -th incremental task */
2  $T_{target} = \text{TempOpt}(\mathcal{D}_{t,valid}, \theta)$ 
3  $\mu = \{\mu_1, \mu_2, \dots, \mu_{C_{t,old}+C_t}\}$ , where
    $\mu_c = \frac{1}{|X_c|} \sum_{\mathbf{x}_e \in X_c} \phi_v(\mathbf{x}_e)$ 
4  $\mathcal{M}_{t,new} = \{(\mathbf{x}_e, y_e) \mid (\mathbf{x}_e, y_e) \in \mathcal{M}_t, y_e \in \mathcal{Y}_t\}$ 
5  $\epsilon_{adv} = \text{MagSearch}(\theta, \mathcal{M}_{t,new}, T_{target}, \mu, \delta)$ 
6  $\mathcal{M}_t^{\epsilon_{adv}} = \{ \}$ 
7 for  $(\mathbf{x}_e, y_e) \in \mathcal{M}_t$  do
   8    $y'_e = \begin{cases} \arg \max_{c: \mu_c \in \mu, c \neq y_e} \|\phi_v(\mathbf{x}_e) - \mu_c\| & \text{if } y_e \in \mathcal{Y}_t \\ \arg \min_{c: \mu_c \in \mu, c \neq y_e} \|\phi_v(\mathbf{x}_e) - \mu_c\| & \text{if } y_e \notin \mathcal{Y}_t \end{cases}$ 
   9    $\mathbf{x}_e^{adv} = \mathbf{x}_e - \epsilon_{adv} \text{sign}(\nabla_{\mathbf{x}_e} \mathcal{L}_{CE}(\mathbf{x}_e, y'_e; \theta))$ 
  10   $\mathcal{M}_t^{\epsilon_{adv}} \leftarrow \mathcal{M}_t^{\epsilon_{adv}} \cup \{(\mathbf{x}_e^{adv}, y_e)\}$ 
11  $T_{adv} = \text{TempOpt}(\mathcal{M}_t^{\epsilon_{adv}}, \theta)$ 
Output:  $T_{adv}$ 
```

which itself is obtained by splitting the whole new-task data \mathcal{D}_t into a training set, $\mathcal{D}_{t,train}$, and a validation set, $\mathcal{D}_{t,valid}$.

Since the increase in ϵ leads to more incorrect predictions by the model, resulting in higher optimized temperatures, we adopt a binary search algorithm to identify the ϵ_{adv} . We denote the perturbed new task exemplar set with magnitude ϵ as $\mathcal{M}_{t,new}^\epsilon$. The ϵ_{adv} value is determined as follows:

$$\epsilon_{adv} = \arg \min_{\epsilon} \|T_{target} - T_{adv}(\epsilon)\| \quad (9)$$

$$T_{target} = \arg \min_T \mathcal{L}_{CE}(\mathbf{x}_v, y_v; \theta, T) \quad (10)$$

$$T_{adv}(\epsilon) = \arg \min_T \mathcal{L}_{CE}(\mathbf{x}_e^{adv}, y_e; \theta, T) \quad (11)$$

where $(\mathbf{x}_v, y_v) \in \mathcal{D}_{t,valid}$ and $(\mathbf{x}_e^{adv}, y_e) \in \mathcal{M}_{t,new}^\epsilon$.

5.3. Overall Algorithm

Algorithm 1 presents the overall procedure of T-CIL, which is designed for class-incremental learning scenarios with multiple tasks. Initially, we determine the target temperature on $\mathcal{D}_{t,valid}$ using Algorithm 3 (TempOpt, detailed in Appendix) (Line 2). We compute the mean of features for all classes, including both old and new task classes (Line 3). We sample the new task exemplar set, $\mathcal{M}_{t,new}$ from \mathcal{M}_t (Line 4). Subsequently, we employ the binary search algorithm described in Algorithm 2 (MagSearch, detailed in Appendix) to determine ϵ_{adv} on $\mathcal{M}_{t,new}$ (Line 5). Using ϵ_{adv} and our perturbation direction policy, we perturb all exemplars (Lines 6–10). Finally, we optimize the temperature on the perturbed exemplar set using Algorithm 3 (Line

11). This optimized temperature will be used for scaling the output logits of the model.

We also analyze the computational complexity of T-CIL. Typical class-incremental learning methods have a complexity of $O(T(N_{new} + M))$, where T is the number of tasks, N_{new} is the number of new task data points, and M is the memory size. T-CIL itself has a complexity of $O(M)$ as its temperature optimization, feature means calculation, perturbation magnitude search, and memory update takes $O(M)$ time (see Appendix for details). Therefore, when combining T-CIL with class-incremental learning methods, the overall complexity remains asymptotically unchanged as M is fixed and significantly smaller than N_{new} .

6. Experiments

We provide experimental results for T-CIL, evaluating the calibration performance of classifiers in a class-incremental learning setting. We report the results with the mean and the standard deviation (\pm in tables) for five random seeds. We use PyTorch [32] with NVIDIA GeForce RTX 4090 GPUs for all experiments.

Metrics We report the top-1 Accuracy, Expected Calibration Error (ECE), and Adaptive Expected Calibration Error (AECE) in percentages. ECE [28] is defined as $\sum_{i=1}^B \frac{|B_i|}{N} |acc(B_i) - conf(B_i)|$, where $acc(B_i)$ is the average accuracy, $conf(B_i)$ is the average confidence of each bin B_i , and N is the number of test data. We use $B = 10$ bins. AECE [27] is another metric for calibration performance evaluation with uniform number of samples for each bin. AECE is also defined as $\sum_{i=1}^B \frac{|B_i|}{N} |acc(B_i) - conf(B_i)|$, but each bin contains $\frac{N}{B}$ samples uniformly, sorted by ascending order of the confidence level. Similar to how taking the average accuracy across tasks is a main metric for class-incremental learning, we take the average calibration error such as average ECE across tasks as a calibration performance metric for class-incremental learning.

Datasets We evaluate our method on three widely used benchmarks for class-incremental learning: CIFAR-10, CIFAR-100, and Tiny-ImageNet. CIFAR-10 and CIFAR-100 [19] share similar characteristics, both consisting of 32×32 RGB images. CIFAR-10 consists of 10 object classes with 5,000 training and 1,000 test images per class, totaling 50,000 training and 10,000 test images. Similarly, CIFAR-100 contains 100 classes, but with fewer images per class: 500 for training and 100 for testing, maintaining the same total of 50,000 training and 10,000 test images. Tiny-ImageNet [22], a compact version of ImageNet ILSVRC 2021 [35], contains 200 classes of 64×64 RGB images, with 500 training, and 50 test images per class.

Table 1. T-CIL performance compared to the five baseline methods on three datasets.

Method	CIFAR-10			CIFAR-100			Tiny-ImageNet		
	Acc. (\uparrow)	ECE (\downarrow)	AECE (\downarrow)	Acc. (\uparrow)	ECE (\downarrow)	AECE (\downarrow)	Acc. (\uparrow)	ECE (\downarrow)	AECE (\downarrow)
Vanilla	65.61 \pm 0.49	28.16 \pm 0.33	28.12 \pm 0.32	56.51 \pm 0.37	27.66 \pm 0.29	27.64 \pm 0.28	31.95 \pm 0.54	32.56 \pm 0.36	32.55 \pm 0.35
TS	65.86 \pm 0.09	23.97 \pm 0.82	23.92 \pm 0.81	56.25 \pm 0.62	16.28 \pm 0.32	16.22 \pm 0.37	31.48 \pm 0.39	19.44 \pm 0.75	19.44 \pm 0.75
ETS	65.86 \pm 0.09	22.46 \pm 1.20	22.39 \pm 1.21	56.25 \pm 0.62	16.83 \pm 0.47	16.80 \pm 0.49	31.48 \pm 0.39	19.81 \pm 0.65	19.83 \pm 0.65
IRM	65.86 \pm 0.09	22.09 \pm 1.73	21.83 \pm 1.73	56.25 \pm 0.62	17.50 \pm 0.64	17.39 \pm 0.61	31.48 \pm 0.39	19.77 \pm 0.72	19.73 \pm 0.78
PerturbTS	n/a	n/a	n/a	56.25 \pm 0.62	16.49 \pm 2.19	16.49 \pm 2.18	31.48 \pm 0.39	10.60 \pm 0.60	10.58 \pm 0.61
T-CIL	65.86 \pm 0.09	17.70\pm2.60	17.64\pm2.59	56.25 \pm 0.62	5.74\pm0.53	5.75\pm0.50	31.48 \pm 0.39	8.12\pm0.38	8.12\pm0.41

Table 2. T-CIL performance combined with four existing class-incremental learning techniques on three datasets.

Method	CIFAR-10			CIFAR-100			Tiny-ImageNet		
	Acc. (\uparrow)	ECE (\downarrow)	AECE (\downarrow)	Acc. (\uparrow)	ECE (\downarrow)	AECE (\downarrow)	Acc. (\uparrow)	ECE (\downarrow)	AECE (\downarrow)
ER	65.61 \pm 0.49	28.16 \pm 0.33	28.12 \pm 0.32	56.51 \pm 0.37	27.66 \pm 0.29	27.64 \pm 0.28	31.95 \pm 0.54	32.56 \pm 0.36	32.55 \pm 0.35
ER+T-CIL	65.86 \pm 0.09	17.70\pm2.60	17.64\pm2.59	56.25 \pm 0.62	5.74\pm0.53	5.75\pm0.50	31.48 \pm 0.39	8.12\pm0.38	8.12\pm0.41
EEIL	77.67 \pm 0.74	15.48 \pm 0.75	15.45 \pm 0.74	60.61 \pm 0.33	21.96 \pm 0.29	21.94 \pm 0.28	37.44 \pm 0.85	29.69 \pm 0.36	29.68 \pm 0.36
EEIL+T-CIL	76.91 \pm 1.27	10.49\pm2.34	10.46\pm2.32	60.74 \pm 0.37	10.30\pm1.10	10.22\pm1.06	37.16 \pm 0.91	15.58\pm0.76	15.56\pm0.76
WA	73.06 \pm 0.57	19.10 \pm 0.50	19.07 \pm 0.51	64.34 \pm 0.40	8.89 \pm 0.64	8.86 \pm 0.63	39.66 \pm 0.88	10.97\pm0.41	10.96\pm0.43
WA+T-CIL	72.75 \pm 0.47	15.61\pm0.23	15.58\pm0.22	64.02 \pm 0.06	3.87\pm0.52	3.84\pm0.55	38.59 \pm 0.44	11.43 \pm 1.00	11.46 \pm 1.04
DER	74.53 \pm 0.48	21.81 \pm 0.46	21.78 \pm 0.47	69.98 \pm 0.69	22.38 \pm 0.37	22.35 \pm 0.35	46.62 \pm 2.84	39.00 \pm 1.72	38.99 \pm 1.72
DER+T-CIL	74.93 \pm 0.35	12.70\pm1.35	12.68\pm1.34	69.98 \pm 0.58	4.37\pm0.59	4.34\pm0.60	47.79 \pm 0.47	6.91\pm0.86	6.90\pm0.84

Experimental Settings For CIFAR-10, we employ a 32-layer ResNet architecture (ResNet-32) [14]. We divide the dataset into 5 incremental tasks, with 2 classes per task. We maintain a memory of 200 samples and use a batch size of 128. For CIFAR-100, we also utilize ResNet-32 and construct the learning with 10 incremental tasks, each containing 10 classes. The memory size is 2,000 samples and the batch size is 128. For Tiny-ImageNet, we adopt ResNet-18 and organize the learning into 10 incremental tasks with 20 classes per task. The memory size is 4,000 samples, and we use the batch size of 256.

Across all datasets, we apply data augmentation techniques including random cropping and horizontal flipping. We utilize maximum memory storage from the initial task to the last task. For all experiments, we train a model for 200 epochs using the Adam [18] optimizer with a weight decay of 0.0002 and use an initial learning rate of 0.1, which is divided by a factor of 10 at epochs 100 and 150.

Baselines We compare T-CIL to existing post-hoc calibration methods adaptable to class-incremental learning settings as baselines: 1) *Vanilla* is a class-incremental learning technique without any calibration method; 2) *TS* [13] is a temperature scaling; 3) *ETS* [44] is an ensemble temperature scaling balancing between calibrated and uncalibrated logits; 4) *IRM* [44] is a multi-class isotonic regression method; 5) *PerturbTS* [37] is an improved temperature

scaling method using a perturbed validation set. Since we do not have a validation set from old tasks, T-CIL and the baselines above only use a validation set from the new task.

6.1. Calibration Results

We compare the overall calibration performance of T-CIL with the five baselines on three datasets as shown in Table 1. We use ER [6] as a base class-incremental learning method. For post-hoc calibration baselines except *Vanilla*, we use 500 samples as a validation set for the new task. While simple calibration methods can improve model calibration in class-incremental learning, T-CIL achieves substantially better calibration performance across three datasets. Specifically, on the CIFAR-100, T-CIL shows remarkable improvement with a 65.2% reduction in calibration error compared to the best post-hoc calibration baselines. The improvements are also significant for other datasets, with 20.0% and 23.4% reductions in calibration error on the CIFAR-10 and Tiny-ImageNet, respectively, compared to the best performing baselines. The ‘n/a’ in Table 1 for *PerturbTS* on the CIFAR-10 indicates that the method is not applicable to this dataset due to the limited number of classes per task (see details in the Appendix).

6.2. Compatibility with CIL Techniques

We evaluate the overall performance of T-CIL when combining class-incremental learning techniques in Table 2. Since T-CIL is a post-hoc calibration method, T-CIL can

Table 3. T-CIL performance compared to the three alternative perturbation direction policies on the CIFAR-100.

Method	Acc. (\uparrow)	ECE (\downarrow)	AECE (\downarrow)
Random class	56.25 ± 0.62	15.09 ± 0.54	15.05 ± 0.59
Closest class only	56.25 ± 0.62	16.39 ± 0.73	16.32 ± 0.71
Farthest class only	56.25 ± 0.62	14.52 ± 0.45	14.49 ± 0.46
T-CIL	56.25 ± 0.62	5.74 ± 0.53	5.75 ± 0.50

be integrated with any existing class-incremental learning technique alleviating catastrophic forgetting including ER [6], EEIL [3], WA [45], and DER [39]. ER is a basic experience replay approach, EEIL and WA are based on knowledge distillation, and DER dynamically expands its architecture as the tasks progress. All methods utilize the memory. For details about experimental settings for each learning techniques including the new-task validation set size, please refer to the Appendix.

Consequently, T-CIL improves the calibration performance across class-incremental learning techniques, which show poor calibration due to their focus on accuracy. While DER achieves the best accuracy on the CIFAR-100 and Tiny-ImageNet, it exhibits the highest calibration error among the techniques. When integrated with DER, T-CIL reduces calibration error by 80.5% and 82.3% on these datasets, respectively. These substantial improvements across different techniques demonstrate T-CIL’s versatility as a general calibration solution for class-incremental learning. When combined with WA, T-CIL shows varying performances across datasets. While achieving significant calibration improvements on the CIFAR-10 and CIFAR-100, it shows slightly higher calibration error than vanilla WA on the Tiny-ImageNet, likely due to WA’s implicit logit scaling for the new task. Nevertheless, the overall benefits of T-CIL across different techniques and datasets demonstrate its effectiveness as a general calibration solution.

We also present the progression of ECE across tasks on CIFAR-100 and Tiny-ImageNet of vanilla, T-CIL, and Optimal TS when combined with four class-incremental learning techniques in the Appendix. When combined with various class-incremental learning techniques, T-CIL consistently demonstrates strong calibration performance across all tasks, with calibration errors approaching Optimal TS’s ideal performance (see details in the Appendix).

6.3. Varying Perturbation Direction Policy

To demonstrate the effectiveness of the perturbation direction policy of T-CIL, we compare it against three possible policy types: (1) *Random class*; (2) *Closest class only*; and (3) *Farthest class only*. ER is used as the base learning method. As shown in Table 3, T-CIL is the only effective approach outperforming other policies that exhibit similar calibration performances with post-hoc calibration

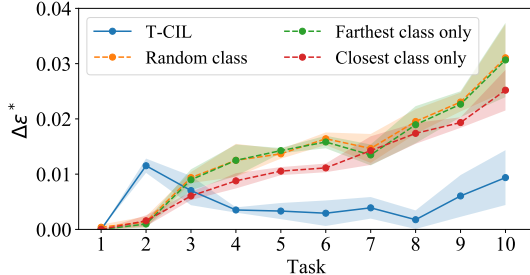


Figure 5. The optimal perturbation magnitude differences ($\Delta\epsilon^*$) on the CIFAR-100 test sets after training each task, comparing the gap between old and new tasks versus new tasks only. Results are presented for the perturbation direction policies of T-CIL and three alternative policies.

baselines. These results demonstrate that the perturbation direction policy of T-CIL is essential for achieving effective calibration in class-incremental learning settings.

We demonstrate that our policy makes ϵ_{adv} determined from only the new-task validation set sufficient to calibrate both old and new tasks. We analyze the optimal perturbation magnitude differences (i.e., $\Delta\epsilon^* = |\epsilon_{old,new}^* - \epsilon_{new}^*|$) on the CIFAR-100, where $\epsilon_{old,new}^*$ and ϵ_{new}^* are searched from both old and new task test sets and only the new task test set, respectively. The optimal magnitude is determined when the temperature calculated on the perturbed exemplars matches the optimal temperature on that set. As shown in Figure 5, our proposed perturbation direction policy maintains small magnitude differences consistently, while other policies show strictly increasing differences, as the tasks progress. This demonstrates that our method can effectively calibrate the model on both old and new tasks using a single ϵ_{adv} from only the new-task validation set.

7. Conclusion

We proposed T-CIL, a novel and effective post-hoc calibration approach tailored to class-incremental learning settings. The existing post-hoc calibration methods are not designed to consider class-incremental learning settings, where validation data of old tasks is limited. T-CIL leverages exemplars for calibration by applying adversarial perturbation to an exemplar set and optimizing the temperature on the perturbed set. The perturbation strategy consists of two key components: direction and magnitude. We determine the magnitude from the new-task validation set and strategically adjust the perturbation direction by guiding the model to misclassify old task samples into their closest classes while directing new task samples into their farthest classes, creating a balanced difficulty in misprediction. We conducted extensive experiments, which showed that T-CIL significantly outperforms post-hoc calibration baselines. We also showed how T-CIL is compatible with various existing learning techniques and improves their calibration performances.

References

- [1] Rahaf Aljundi, Eugene Belilovsky, Tinne Tuytelaars, Laurent Charlin, Massimo Caccia, Min Lin, and Lucas Page-Caccia. Online continual learning with maximal interfered retrieval. *Advances in Neural Information Processing Systems*, 32, 2019. 3
- [2] Nicholas Carlini and David Wagner. Towards evaluating the robustness of neural networks. In *2017 IEEE Symposium on Security and Privacy (SP)*, pages 39–57. IEEE, 2017. 5
- [3] Francisco M Castro, Manuel J Marín-Jiménez, Nicolás Guil, Cordelia Schmid, and Karteek Alahari. End-to-end incremental learning. In *Proceedings of the European Conference on Computer Vision*, pages 233–248, 2018. 1, 2, 3, 8, 4
- [4] Gert Cauwenberghs and Tomaso Poggio. Incremental and decremental support vector machine learning. *Advances in Neural Information Processing Systems*, 13, 2000. 3
- [5] Arslan Chaudhry, Marc’Aurelio Ranzato, Marcus Rohrbach, and Mohamed Elhoseiny. Efficient lifelong learning with a gem. *arXiv preprint arXiv:1812.00420*, 2018. 3
- [6] Arslan Chaudhry, Marcus Rohrbach, Mohamed Elhoseiny, Thalaiyasingam Ajanthan, Puneet K Dokania, Philip HS Torr, and Marc’Aurelio Ranzato. On tiny episodic memories in continual learning. *arXiv preprint arXiv:1902.10486*, 2019. 2, 3, 4, 7, 8
- [7] Muthu Chidambaram and Rong Ge. On the limitations of temperature scaling for distributions with overlaps. *International Conference on Learning Representations*, 2024. 3
- [8] Wonjeong Choi, Jungwuk Park, Dong-Jun Han, Younghyun Park, and Jaekyun Moon. Consistency-guided temperature scaling using style and content information for out-of-domain calibration. *arXiv preprint arXiv:2402.15019*, 2024. 3
- [9] Zhipeng Ding, Xu Han, Peirong Liu, and Marc Niethammer. Local temperature scaling for probability calibration. In *Proceedings of the IEEE/CVF International Conference on Computer Vision*, pages 6889–6899, 2021. 3
- [10] Arindam Ghosh, Thomas Schaaf, and Matthew Gormley. Adafocal: Calibration-aware adaptive focal loss. *Advances in Neural Information Processing Systems*, 35:1583–1595, 2022. 2
- [11] Ian J Goodfellow, Jonathon Shlens, and Christian Szegedy. Explaining and harnessing adversarial examples. *arXiv preprint arXiv:1412.6572*, 2014. 4, 5
- [12] Sorin Grigorescu, Bogdan Trusnea, Tiberiu Cocias, and Gigel Macesanu. A survey of deep learning techniques for autonomous driving. *Journal of field robotics*, 37(3):362–386, 2020. 1
- [13] Chuan Guo, Geoff Pleiss, Yu Sun, and Kilian Q Weinberger. On calibration of modern neural networks. In *International Conference on Machine Learning*, pages 1321–1330. PMLR, 2017. 1, 3, 7, 4
- [14] Kaiming He, Xiangyu Zhang, Shaoqing Ren, and Jian Sun. Deep residual learning for image recognition. In *Proceedings of the IEEE conference on Computer Vision and Pattern Recognition*, pages 770–778, 2016. 4, 7
- [15] Xiaoqian Jiang, Melanie Osl, Jihoon Kim, and Lucila Ohno-Machado. Calibrating predictive model estimates to support personalized medicine. *Journal of the American Medical Informatics Association*, 19(2):263–274, 2012. 1
- [16] Tom Joy, Francesco Pinto, Ser-Nam Lim, Philip HS Torr, and Puneet K Dokania. Sample-dependent adaptive temperature scaling for improved calibration. In *Proceedings of the AAAI Conference on Artificial Intelligence*, pages 14919–14926, 2023. 3
- [17] Dongmin Kang, Yeonsik Jo, Yeongwoo Nam, and Jonghyun Choi. Confidence calibration for incremental learning. *IEEE Access*, 8:126648–126660, 2020. 3
- [18] Diederik P Kingma. Adam: A method for stochastic optimization. *arXiv preprint arXiv:1412.6980*, 2014. 7
- [19] Alex Krizhevsky, Geoffrey Hinton, et al. Learning multiple layers of features from tiny images. 2009. 6
- [20] Meelis Kull, Miquel Perello Nieto, Markus Kängsepp, Telmo Silva Filho, Hao Song, and Peter Flach. Beyond temperature scaling: Obtaining well-calibrated multi-class probabilities with dirichlet calibration. *Advances in Neural Information Processing Systems*, 32, 2019. 3
- [21] Ilja Kuzborskij, Francesco Orabona, and Barbara Caputo. From n to n+1: Multiclass transfer incremental learning. In *Proceedings of the IEEE Conference on Computer Vision and Pattern Recognition*, 2013. 3
- [22] Ya Le and Xuan Yang. Tiny imagenet visual recognition challenge. *CS 231N*, 7(7):3, 2015. 6
- [23] Lanpei Li, Elia Piccoli, Andrea Cossu, Davide Bacciu, and Vincenzo Lomonaco. Calibration of continual learning models. In *Proceedings of the IEEE/CVF Conference on Computer Vision and Pattern Recognition Workshop (CVPRW)*, pages 4160–4169, 2024. 3
- [24] Bingyuan Liu, Ismail Ben Ayed, Adrian Galdran, and Jose Dolz. The devil is in the margin: Margin-based label smoothing for network calibration. In *Proceedings of the IEEE/CVF Conference on Computer Vision and Pattern Recognition*, pages 80–88, 2022. 2
- [25] David Lopez-Paz and Marc’Aurelio Ranzato. Gradient episodic memory for continual learning. *Advances in Neural Information Processing Systems*, 30, 2017. 1, 3
- [26] Michael McCloskey and Neal J Cohen. Catastrophic interference in connectionist networks: The sequential learning problem. In *Psychology of learning and motivation*, pages 109–165. Elsevier, 1989. 1
- [27] Jishnu Mukhoti, Viveka Kulharia, Amartya Sanyal, Stuart Golodetz, Philip Torr, and Puneet Dokania. Calibrating deep neural networks using focal loss. *Advances in Neural Information Processing Systems*, 33:15288–15299, 2020. 1, 2, 6
- [28] Mahdi Pakdaman Naeini, Gregory Cooper, and Milos Hauskrecht. Obtaining well calibrated probabilities using bayesian binning. In *Proceedings of the AAAI conference on artificial intelligence*, 2015. 3, 6
- [29] Jongyoun Noh, Hyekang Park, Junghyup Lee, and Bumsuh Ham. Rankmixup: Ranking-based mixup training for network calibration. In *Proceedings of the IEEE/CVF International Conference on Computer Vision*, pages 1358–1368, 2023. 2
- [30] Yaniv Ovadia, Emily Fertig, Jie Ren, Zachary Nado, David Sculley, Sebastian Nowozin, Joshua Dillon, Balaji Lakshminarayanan, and Jasper Snoek. Can you trust your model’s

- uncertainty? evaluating predictive uncertainty under dataset shift. *Advances in Neural Information Processing Systems*, 32, 2019. 3
- [31] Hyekang Park, Jongyoun Noh, Youngmin Oh, Donghyeon Baek, and Bumsu Ham. Acls: Adaptive and conditional label smoothing for network calibration. In *Proceedings of the IEEE/CVF International Conference on Computer Vision*, pages 3936–3945, 2023. 2
- [32] Adam Paszke, Sam Gross, Francisco Massa, Adam Lerer, James Bradbury, Gregory Chanan, Trevor Killeen, Zeming Lin, Natalia Gimelshein, Luca Antiga, et al. Pytorch: An imperative style, high-performance deep learning library. *Advances in Neural Information Processing Systems*, 32, 2019. 6
- [33] John Platt et al. Probabilistic outputs for support vector machines and comparisons to regularized likelihood methods. *Advances in large margin classifiers*, 10(3):61–74, 1999. 3
- [34] Sylvestre-Alvise Rebuffi, Alexander Kolesnikov, Georg Sperl, and Christoph H Lampert. icarl: Incremental classifier and representation learning. In *Proceedings of the IEEE conference on Computer Vision and Pattern Recognition*, pages 2001–2010, 2017. 1, 3
- [35] Olga Russakovsky, Jia Deng, Hao Su, Jonathan Krause, Sanjeev Satheesh, Sean Ma, Zhiheng Huang, Andrej Karpathy, Aditya Khosla, Michael Bernstein, et al. Imagenet large scale visual recognition challenge. *International journal of computer vision*, 115:211–252, 2015. 6
- [36] Christian Szegedy, Vincent Vanhoucke, Sergey Ioffe, Jon Shlens, and Zbigniew Wojna. Rethinking the inception architecture for computer vision. In *Proceedings of the IEEE conference on Computer Vision and Pattern Recognition*, pages 2818–2826, 2016. 1, 2
- [37] Christian Tomani, Sebastian Gruber, Muhammed Ebrar Erdem, Daniel Cremers, and Florian Buettner. Post-hoc uncertainty calibration for domain drift scenarios. In *Proceedings of the IEEE/CVF Conference on Computer Vision and Pattern Recognition*, pages 10124–10132, 2021. 3, 7, 1, 4
- [38] Yue Wu, Yinpeng Chen, Lijuan Wang, Yuancheng Ye, Zicheng Liu, Yandong Guo, and Yun Fu. Large scale incremental learning. In *Proceedings of the IEEE/CVF conference on Computer Vision and Pattern Recognition*, pages 374–382, 2019. 1, 3
- [39] Shipeng Yan, Jiangwei Xie, and Xuming He. Der: Dynamically expandable representation for class incremental learning. In *Proceedings of the IEEE/CVF conference on Computer Vision and Pattern Recognition*, pages 3014–3023, 2021. 1, 3, 4, 5, 8
- [40] Yaodong Yu, Stephen Bates, Yi Ma, and Michael Jordan. Robust calibration with multi-domain temperature scaling. *Advances in Neural Information Processing Systems*, 35: 27510–27523, 2022. 3
- [41] Bianca Zadrozny and Charles Elkan. Obtaining calibrated probability estimates from decision trees and naive bayesian classifiers. In *International Conference on Machine Learning*, pages 609–616, 2001. 1, 3
- [42] Bianca Zadrozny and Charles Elkan. Transforming classifier scores into accurate multiclass probability estimates. In *Proceedings of the eighth ACM SIGKDD international conference on Knowledge discovery and data mining*, pages 694–699, 2002. 3
- [43] Hongyi Zhang, Moustapha Cissé, Yann N. Dauphin, and David Lopez-Paz. mixup: Beyond empirical risk minimization. In *International Conference on Learning Representations*, 2018. 1, 2
- [44] Jize Zhang, Bhavya Kailkhura, and T Han. Mix-n-match: Ensemble and compositional methods for uncertainty calibration in deep learning. In *International Conference on Machine Learning*, 2020. 3, 7, 4
- [45] Bowen Zhao, Xi Xiao, Guojun Gan, Bin Zhang, and Shu-Tao Xia. Maintaining discrimination and fairness in class incremental learning. In *Proceedings of the IEEE/CVF conference on Computer Vision and Pattern Recognition*, pages 13208–13217, 2020. 3, 8, 1, 4
- [46] Da-Wei Zhou, Qi-Wei Wang, Zhi-Hong Qi, Han-Jia Ye, De-Chuan Zhan, and Ziwei Liu. Deep class-incremental learning: A survey. *arXiv preprint arXiv:2302.03648*, 2023. 1, 3
- [47] Zhi-Hua Zhou, Jianxin Wu, and Wei Tang. Ensembling neural networks: many could be better than all. *Artificial intelligence*, 137(1-2):239–263, 2002. 3

T-CIL: Temperature Scaling using Adversarial Perturbation for Calibration in Class-Incremental Learning

Supplementary Material

1. Detailed Algorithms

We provide full algorithms of Algorithm 2 (MagSearch) for magnitude search, and Algorithm 3 (TempOpt) for temperature optimization.

Algorithm 2: The magnitude search algorithm for perturbation (MagSearch).

Input: Model parameters $\theta = \{w, v\}$, exemplar set from new task $\mathcal{M}_{t,new}$, target temperature T_{target} , set of feature means μ , tolerance δ

```
1  $\epsilon_{low} \leftarrow 0.0, \epsilon_{high} \leftarrow 1.0$ 
2 while  $\epsilon_{high} - \epsilon_{low} > \delta$  do
3    $\epsilon = \frac{\epsilon_{low} + \epsilon_{high}}{2.0}$ 
4    $\mathcal{M}_{t,new}^\epsilon = \{ \}$ 
5   for  $(\mathbf{x}_e, y_e) \in \mathcal{M}_{t,new}$  do
6      $y'_e = \arg \max_{c: \mu_c \in \mu, c \neq y_e} \|\phi_v(\mathbf{x}_e) - \mu_c\|$ 
7      $\mathbf{x}_e^{adv} = \mathbf{x}_e - \epsilon \text{sign}(\nabla_{\mathbf{x}_e} \mathcal{L}_{CE}(\mathbf{x}_e, y'_e; \theta))$ 
8      $\mathcal{M}_{t,new}^\epsilon \leftarrow \mathcal{M}_{t,new}^\epsilon \cup \{(\mathbf{x}_e^{adv}, y_e)\}$ 
9    $T = \text{TempOpt}(\mathcal{M}_{t,new}^\epsilon, \theta)$ 
10  if  $T < T_{target}$  then
11     $\epsilon_{low} \leftarrow \epsilon$ 
12  else
13     $\epsilon_{high} \leftarrow \epsilon$ 
```

Output: $\frac{\epsilon_{low} + \epsilon_{high}}{2.0}$

Algorithm 3: The temperature optimization algorithm (TempOpt).

Input: Dataset \mathcal{D} , model parameters θ

```
1  $T \leftarrow 1$ ; // Initialize  $T$ 
2 while not converge do
3   for  $(\mathbf{x}, y) \in \mathcal{D}$  do
4     Update  $T$  to minimize  $\mathcal{L}_{CE}(\mathbf{x}, y; \theta, T)$ 
```

Output: T

2. Computational Complexity Analysis

In this section, we analyze the computational complexity of T-CIL. T-CIL consists of four main components: temperature optimization, feature means calculation, perturbation magnitude search, and memory update. The complexity of temperature optimization is $O(M)$, where M represents the

memory size, since we optimize the temperature on the set of perturbed exemplars for memory. Similarly, calculating feature means requires $O(M)$ operations. The adversarial search process takes $O(M)$ time (with a constant factor k for perturbation iterations), and applying perturbations also has a complexity of $O(M)$. Therefore, the overall computational complexity of T-CIL for a single incremental task is also $O(M)$.

As conventional class-incremental learning approaches operate with $O(T(N_{new} + M))$ complexity, T-CIL maintains a lighter $O(M)$ complexity, where T is the number of tasks, N_{new} is the number of new task data points, and M is the memory size. Consequently, integrating T-CIL with existing class-incremental frameworks preserves the asymptotic computational efficiency, as M remains constant and substantially less than N_{new} . With a small overhead, T-CIL is an efficient approach that can be practically combined with existing class-incremental learning methods.

3. Experiments

3.1. Inapplicability of PerturbTS on the CIFAR-10

The reason PerturbTS [37] is not applicable on the CIFAR-10 in a class-incremental learning setup is that, with only two new classes per task, the model quickly fits to the data, making it impossible to achieve the designated accuracy reduction through perturbation. This overfitting prevents the perturbation magnitude optimization from converging.

3.2. Detailed Experimental Settings

To obtain the best calibration performance of T-CIL with the minimal impact on accuracy, we use a new-task validation set whose size varies depending on the class-incremental learning technique and dataset used. The new-task validation set sizes are listed in Table 4. The effect of the new-task validation set size will be explained later.

Class-incremental learning techniques require specific training parameters. For both EEIL [3] and WA [45], we set the knowledge distillation temperature to 2. EEIL and DER [39] incorporate a balanced fine-tuning phase. For this phase, we train the model for 30 epochs with 10 tasks and 100 epochs with 20 tasks.

After model training, we store a subset of new-task data used for training to the memory by uniformly sampling exemplars from each class. As the memory size is fixed, we remove some existing exemplars to accommodate the new-task data.

Table 4. The size of the new-task validation set for each class-incremental learning method and dataset used in the main experiments.

Method	CIFAR-10	CIFAR-100	Tiny-ImageNet
ER	500	500	100
EEIL	300	300	200
WA	100	500	100
DER	500	1000	100

We make a fair comparison between post-hoc calibration methods including T-CIL versus vanilla class-incremental learning techniques in terms of training data. In particular, whenever we take a (minimal) validation set from the training data, we only train models on the remaining training data. In comparison, the vanilla techniques always train on the full training set.

3.3. Additional Experiments

Full experimental results We evaluate T-CIL against five calibration baselines (Cal method) in combination with four class-incremental learning techniques (CIL method) across three datasets. Table 5 presents a comprehensive comparison of all possible combinations between post-hoc calibration methods and class-incremental learning techniques.

Overall, T-CIL outperforms the five calibration baselines when integrated with four existing class-incremental learning techniques across three datasets. Notably, T-CIL consistently shows low calibration errors compared to all the baselines. While PerturbTS achieves the best calibration performances when combined with EEIL and WA on the Tiny-ImageNet, its effectiveness is inconsistent. In addition, PerturbTS is not applicable to the CIFAR-10 dataset and exhibits unusually high calibration errors on the CIFAR-100 dataset. In contrast, T-CIL demonstrates robust and superior performances across all experimental settings, consistently achieving lower calibration errors regardless of the underlying class-incremental learning technique. This comprehensive evaluation validates that T-CIL is a more reliable and versatile approach for addressing calibration challenges in class-incremental learning scenarios.

Expansion of incremental tasks We evaluate the performance when expanding incremental tasks from 10 to 20 tasks, with results presented in Table 6. For all class-incremental learning techniques, we use 100 samples from each new task as a validation set on both CIFAR-100 and Tiny-ImageNet.

The results show that T-CIL outperforms most vanilla class-incremental learning techniques, with WA being the only exception. As explained in Section 6.2, WA scales the output logits corresponding to the new task only after train-

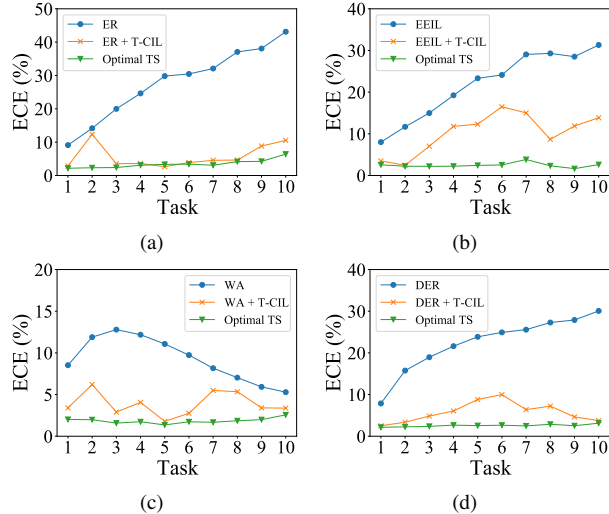


Figure 6. ECE (%) comparison after training each task on the CIFAR-100 among existing class-incremental learning techniques, their combinations with T-CIL, and the optimal TS. The existing techniques include: (a) ER, (b) EEIL, (c) WA, and (d) DER.

ing. This scaling of specific logits may not align with the insight behind T-CIL’s perturbation direction policy. Nevertheless, T-CIL significantly improves the calibration performance of poorly calibrated class-incremental learning techniques.

Varying size of memory We analyze how memory size affects the ECE of T-CIL compared to the vanilla method without calibration on the CIFAR-100 and Tiny-ImageNet, as shown in Figure 7. Using ER as our base class-incremental learning technique, we experiment with memory sizes of 500, 1,000, 1,500, and 2,000 samples for CIFAR-100, and 1,000, 2,000, 3,000, and 4,000 samples for Tiny-ImageNet. We use a new-task validation set sized of 100.

Our results demonstrate that T-CIL consistently achieves significantly lower ECE than the vanilla method across all memory sizes. Although smaller memory sizes lead to decreased model accuracy and consequently worse calibration performance, T-CIL with just 500 memory samples still outperforms the vanilla method using 2,000 samples in terms of calibration quality.

Varying size of new-task validation set We vary the size of the new-task validation set and evaluate ECE and accuracy on CIFAR-100, using ER as a base class-incremental learning technique. We present the results in Figure 8 and Table 7.

Figure 8 demonstrates that T-CIL is effective even with a small-sized validation set. As the validation set size increases, ECE decreases. However, increasing validation set size leads to accuracy drop due to the smaller training set

size. These trends in ECE and accuracy indicate that T-CIL only requires small new-task validation set for calibrating the model effectively while minimizing the impact on accuracy.

Additional ECE progressions We present the progression of ECE across tasks on CIFAR-100 and Tiny-ImageNet of vanilla, T-CIL, and Optimal TS when combined with four class-incremental learning techniques in Figure 6 and Figure 9. These figures show the progression of ECE throughout tasks, where we compare T-CIL against an ideal scenario where we run *TS* on the test set of both old and new tasks and thus obtain the best achievable calibration performance (called “Optimal TS”). When combined with various class-incremental learning techniques, T-CIL consistently demonstrates strong calibration performance across all tasks, with calibration errors approaching Optimal TS’s ideal performance.

Table 5. Performance comparison between T-CIL and five baselines when integrated with four class-incremental learning techniques on three datasets.

CIL Method	Cal Method	CIFAR-10			CIFAR-100			Tiny-ImageNet		
		Acc. (\uparrow)	ECE (\downarrow)	AECE (\downarrow)	Acc. (\uparrow)	ECE (\downarrow)	AECE (\downarrow)	Acc. (\uparrow)	ECE (\downarrow)	AECE (\downarrow)
ER [6]	Vanilla	65.61 \pm 0.49	28.16 \pm 0.33	28.12 \pm 0.32	56.51 \pm 0.37	27.66 \pm 0.29	27.64 \pm 0.28	31.95 \pm 0.54	32.56 \pm 0.36	32.55 \pm 0.35
	TS [13]	65.86 \pm 0.09	23.97 \pm 0.82	23.92 \pm 0.81	56.25 \pm 0.62	16.28 \pm 0.32	16.22 \pm 0.37	31.48 \pm 0.39	19.44 \pm 0.75	19.44 \pm 0.75
	ETS [44]	65.86 \pm 0.09	22.46 \pm 1.20	22.39 \pm 1.21	56.25 \pm 0.62	16.83 \pm 0.47	16.80 \pm 0.49	31.48 \pm 0.39	19.81 \pm 0.65	19.83 \pm 0.65
	IRM [44]	65.86 \pm 0.09	22.09 \pm 1.73	21.83 \pm 1.73	56.25 \pm 0.62	17.50 \pm 0.64	17.39 \pm 0.61	31.48 \pm 0.39	19.77 \pm 0.72	19.73 \pm 0.78
	PerturbTS [37]	n/a	n/a	n/a	56.25 \pm 0.62	16.49 \pm 2.19	16.49 \pm 2.18	31.48 \pm 0.39	10.60 \pm 0.60	10.58 \pm 0.61
	T-CIL	65.86 \pm 0.09	17.70\pm2.60	17.64\pm2.59	56.25 \pm 0.62	5.74\pm0.53	5.75\pm0.50	31.48 \pm 0.39	8.12\pm0.38	8.12\pm0.41
EEIL [3]	Vanilla	77.67 \pm 0.74	15.48 \pm 0.75	15.45 \pm 0.74	60.61 \pm 0.33	21.96 \pm 0.29	21.94 \pm 0.28	37.44 \pm 0.85	29.69 \pm 0.36	29.68 \pm 0.36
	TS	76.91 \pm 1.27	10.20\pm0.94	10.16\pm0.93	60.74 \pm 0.37	13.25 \pm 0.60	13.14 \pm 0.55	37.16 \pm 0.91	13.16 \pm 0.76	13.15 \pm 0.73
	ETS	76.91 \pm 1.27	10.31 \pm 0.71	10.29 \pm 0.72	60.74 \pm 0.37	13.89 \pm 0.47	13.83 \pm 0.42	37.16 \pm 0.91	13.52 \pm 0.73	13.51 \pm 0.71
	IRM	76.91 \pm 1.27	10.51 \pm 0.59	10.32 \pm 0.53	60.74 \pm 0.37	15.20 \pm 0.48	15.09 \pm 0.51	37.16 \pm 0.91	14.66 \pm 0.76	14.69 \pm 0.76
	PerturbTS	n/a	n/a	n/a	60.74 \pm 0.37	40.34 \pm 3.84	40.34 \pm 3.84	37.16 \pm 0.91	8.81\pm0.59	8.81\pm0.61
	T-CIL	76.91 \pm 1.27	10.49 \pm 2.34	10.46 \pm 2.32	60.74 \pm 0.37	10.30\pm1.10	10.22\pm1.06	37.16 \pm 0.91	15.58 \pm 0.76	15.56 \pm 0.76
WA [45]	Vanilla	73.06 \pm 0.57	19.10 \pm 0.50	19.07 \pm 0.51	64.34 \pm 0.40	8.89 \pm 0.64	8.86 \pm 0.63	39.66 \pm 0.88	10.97 \pm 0.41	10.96 \pm 0.43
	TS	72.75 \pm 0.47	18.22 \pm 0.69	18.19 \pm 0.69	64.02 \pm 0.06	5.93 \pm 0.24	5.88 \pm 0.28	38.59 \pm 0.44	13.24 \pm 1.08	13.28 \pm 1.09
	ETS	72.75 \pm 0.47	17.96 \pm 0.67	17.92 \pm 0.69	64.02 \pm 0.06	5.77 \pm 0.39	5.75 \pm 0.42	38.59 \pm 0.44	13.01 \pm 1.12	13.06 \pm 1.12
	IRM	72.75 \pm 0.47	18.03 \pm 0.94	17.58 \pm 0.97	64.02 \pm 0.06	6.61 \pm 0.47	6.51 \pm 0.46	38.59 \pm 0.44	10.88 \pm 0.46	10.87 \pm 0.48
	PerturbTS	n/a	n/a	n/a	64.02 \pm 0.06	46.55 \pm 2.20	46.54 \pm 2.20	38.59 \pm 0.44	8.63\pm1.07	8.61\pm1.10
	T-CIL	72.75 \pm 0.47	15.61\pm0.23	15.58\pm0.22	64.02 \pm 0.06	3.87\pm0.52	3.84\pm0.55	38.59 \pm 0.44	11.43 \pm 1.00	11.46 \pm 1.04
DER [39]	Vanilla	74.53 \pm 0.48	21.81 \pm 0.46	21.78 \pm 0.47	69.98 \pm 0.69	22.38 \pm 0.37	22.35 \pm 0.35	46.62 \pm 2.84	39.00 \pm 1.72	38.99 \pm 1.72
	TS	74.93 \pm 0.35	17.27 \pm 0.37	17.25 \pm 0.37	69.98 \pm 0.58	6.16 \pm 0.25	6.04 \pm 0.26	47.79 \pm 0.47	11.29 \pm 0.66	11.26 \pm 0.66
	ETS	74.93 \pm 0.35	16.82 \pm 0.28	16.79 \pm 0.29	69.98 \pm 0.58	6.12 \pm 0.36	6.03 \pm 0.37	47.79 \pm 0.47	7.83 \pm 0.63	7.86 \pm 0.58
	IRM	74.93 \pm 0.35	17.04 \pm 0.45	16.80 \pm 0.48	69.98 \pm 0.58	7.88 \pm 0.33	8.03 \pm 0.40	47.79 \pm 0.47	10.47 \pm 0.61	11.01 \pm 0.61
	PerturbTS	n/a	n/a	n/a	69.98 \pm 0.58	52.21 \pm 5.97	52.21 \pm 5.97	47.79 \pm 0.47	15.56 \pm 1.18	15.55 \pm 1.18
	T-CIL	74.93 \pm 0.35	12.70\pm1.35	12.68\pm1.34	69.98 \pm 0.58	4.37\pm0.59	4.34\pm0.60	47.79 \pm 0.47	6.91\pm0.86	6.90\pm0.84

Table 6. T-CIL performance combined with four existing class-incremental learning techniques on two datasets, each containing 20 incremental tasks.

Method	CIFAR-100			Tiny-ImageNet		
	Acc. (\uparrow)	ECE (\downarrow)	AECE (\downarrow)	Acc. (\uparrow)	ECE (\downarrow)	AECE (\downarrow)
ER	54.81 \pm 0.70	28.95 \pm 0.84	28.93 \pm 0.84	30.43 \pm 0.51	34.90 \pm 0.16	34.88 \pm 0.16
ER+T-CIL	54.48 \pm 1.95	7.08\pm0.49	7.07\pm0.46	30.62 \pm 0.29	10.72\pm0.88	10.79\pm0.86
EEIL	55.36 \pm 1.19	25.17 \pm 0.84	25.15 \pm 0.84	33.54 \pm 0.60	28.89 \pm 0.27	28.89 \pm 0.27
EEIL+T-CIL	55.86 \pm 0.93	14.38\pm1.34	14.35\pm1.35	34.22 \pm 0.18	24.45\pm0.67	24.46\pm0.67
WA	59.30 \pm 0.64	7.39\pm0.35	7.37\pm0.35	35.99 \pm 0.97	10.06\pm0.95	10.06\pm0.99
WA+T-CIL	58.89 \pm 0.67	7.45\pm0.72	7.47\pm0.72	36.80 \pm 0.42	19.56 \pm 0.47	19.57 \pm 0.48
DER	68.90 \pm 0.31	24.05 \pm 0.45	24.02 \pm 0.45	48.63 \pm 0.75	42.44 \pm 0.56	42.43 \pm 0.56
DER+T-CIL	68.84 \pm 0.61	5.78\pm0.92	5.75\pm0.91	48.33 \pm 1.31	5.90\pm0.97	5.91\pm0.96

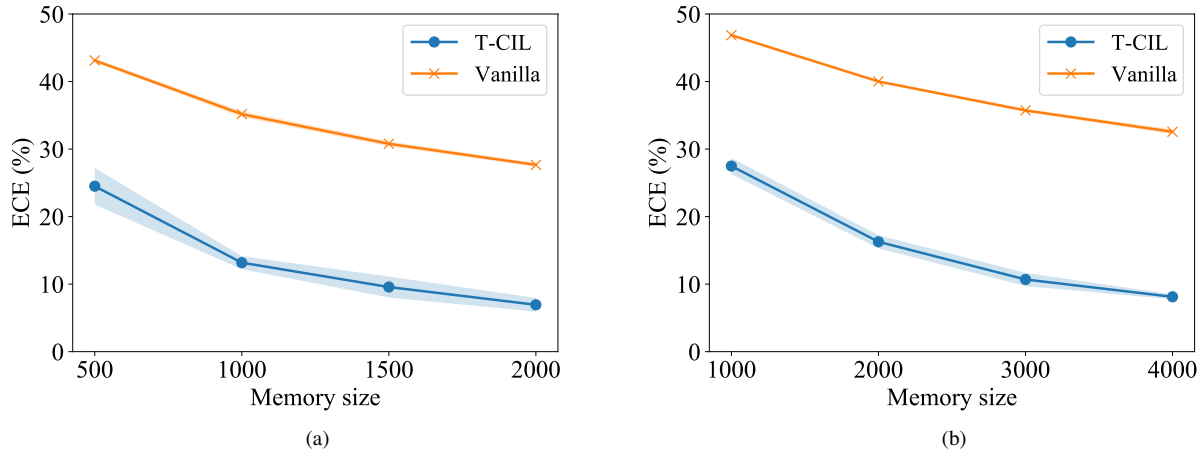


Figure 7. T-CIL performance when varying the memory size on (a) CIFAR-100 and (b) Tiny-ImageNet.

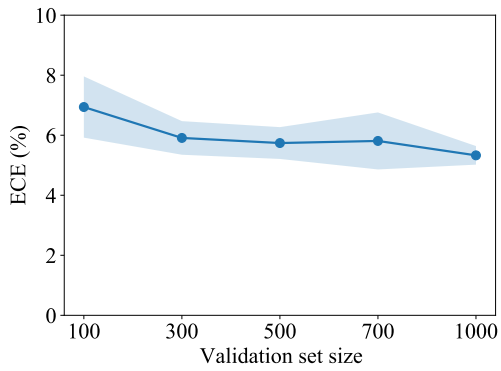


Figure 8. T-CIL performance when varying the size of the new-task validation set on the CIFAR-100.

Table 7. T-CIL performance when varying the size of the new-task validation set on the CIFAR-100.

Val size	100	300	500	700	1000
ECE (%)	6.94 ± 1.02	5.91 ± 0.56	5.74 ± 0.53	5.81 ± 0.95	5.33 ± 0.31
Acc (%)	56.97 ± 0.65	56.95 ± 0.34	56.25 ± 0.62	56.55 ± 0.80	56.08 ± 0.57

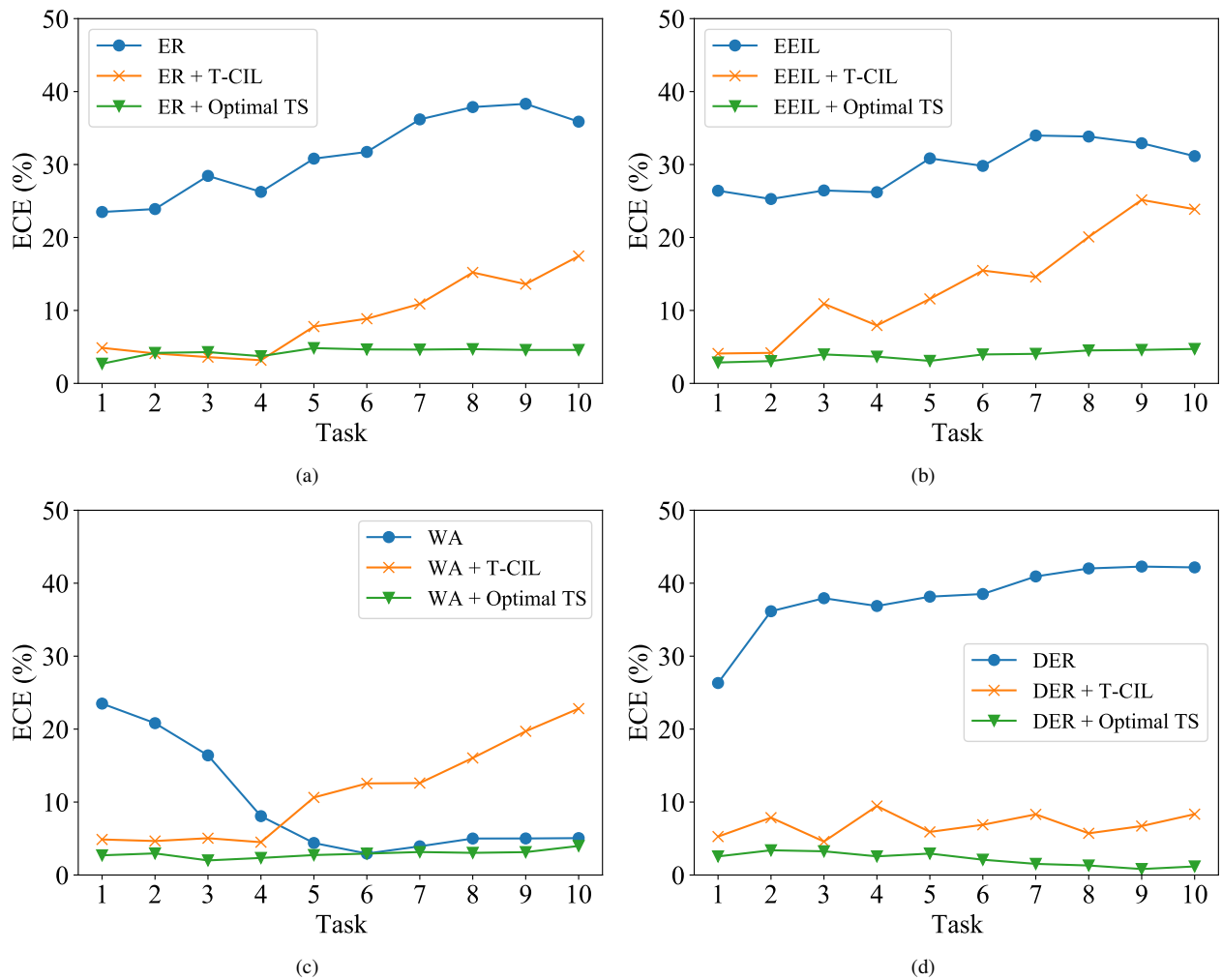


Figure 9. ECE progression after training each task on the Tiny-ImageNet among existing class-incremental learning techniques, their combinations with T-CIL, and the optimal TS. The existing techniques include: (a) ER, (b) EEIL, (c) WA, and (d) DER.